

# Quantum Chaos of Unitary Fermi Gases in Strong Pairing Fluctuation Region

Xinloong Han<sup>1</sup> and Boyang Liu<sup>2,\*</sup>

<sup>1</sup>*Department of Physics and Center of Theoretical and Computational Physics,  
The University of Hong Kong, Hong Kong, China*

<sup>2</sup>*Institute of Theoretical Physics, Beijing University of Technology Beijing 100124, China*  
(Dated: February 9, 2020)

The growth rate of the out-of-time-ordered correlator in a N-flavor Fermi gas is investigated and the Lyapunov exponent  $\lambda_L$  is calculated to the order of  $1/N$ . We find that the Lyapunov exponent monotonically increases as the interaction strength increases from the BCS limit to the unitary region. At the unitarity the Lyapunov exponent increases while the temperature drops and it can reach to the order of  $\lambda_L \sim T$  around the critical temperature for the  $N = 1$  case. The system scrambles faster for stronger pairing fluctuations. At the BCS limit, the Lyapunov exponent behaviors as  $\lambda_L \propto e^{\mu/T} a_s^2 T^2 / N$ .

## I. INTRODUCTION

Information scrambling is a crucial stage in thermalization of a closed system. During this process the quantum entanglement spreads across all the freedoms of the system and the memory of the initial state is lost, which is taken as a key prerequisite for thermalization. Recently, the studies in gauge gravity duality have inspired some new insights into the quantum chaos[1–8]. It is suggested the black holes are the fastest scramblers in nature[1]. Moreover, the experimental realizations of nearly isolated quantum systems also attract increasing attention to this area [9–11]. Analogous to the Lyapunov exponents describing the growth of chaos in classical models, the scrambling to the quantum chaos can also be probed by growth rate of so called out-of-time-ordered correlator (OTOC).

The OTOC was first introduced by A. I. Larkin and Yu. N. Ovchinnikov in the study of superconductivity[12]. Recently, this subject is revived by the discovery of an unexpected bound on the Lyapunov exponent that is extracted from OTOC [1, 13]. Several experiments on measurement of OTOC have been conducted [14–17]. Usually, in stead of directly calculating the OTOC it's more convenient to evaluate the "regulated" squared commutator defined  $\mathcal{C}(t) = \text{Tr}\{\sqrt{\rho}[W(t), V(0)]^\dagger \sqrt{\rho}[W(t), V(0)]\}$  [18, 19], where  $\rho = e^{-\beta H}$  is the thermal density matrix and  $W$  and  $V$  are local Hermitian operators in general. It can be expanded as  $\mathcal{C}(t) = 2\text{Tr}\{\sqrt{\rho}W(t)V(0)\sqrt{\rho}V(0)W(t)\} - 2\text{Re}[\text{Tr}\{\sqrt{\rho}W(t)V(0)\sqrt{\rho}W(t)V(0)\}]$ . The first term is time ordered. On the other hand, the second term is on an unusual time order as illustrated in Fig. 1 and it's called OTOC. In a chaotic system  $\mathcal{C}(t)$  is expected to have an exponential behavior at the time scale  $t_L$  as  $\mathcal{C}(t) \sim e^{\lambda_L t}$ . Analogous to the classical chaos,  $\lambda_L$  is called Lyapunov exponent and  $t_L^{-1} \sim \lambda_L$ . Based on some reasonable physical assumption, Lyapunov exponent is proven to have an upper bound of  $2\pi k_B T / \hbar$  and

it saturates in models with gravity duals[1, 13]. A concrete example is the celebrated Sachdev-Ye-Kitaev (SYK) model[20–22] which holds a conformal symmetry in the low-energy limit and is dual to an  $\text{AdS}_2$  gravity theory.

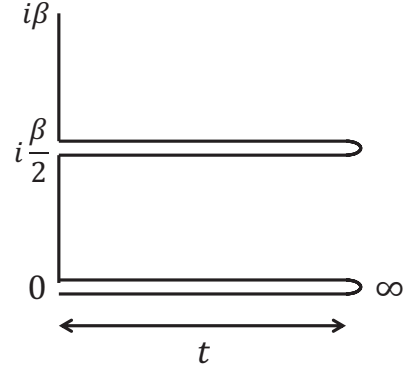


FIG. 1. The complex time contour for calculating the out-of-time-ordered correlators. The horizontal direction represents the real time evolution and the vertical direction represents the imaginary time evolution. It contains two real time folds, which are separated by  $i\beta/2$ .

In condensed matter physics, the systems usually don't possess conformal symmetry. However, there exist some exceptions. At the critical point the conformal symmetry can emerge for low energy and long distance. Investigations have been done in this regime [19, 23, 24]. In these system there are no quasi-particle excitations and the temperature is the only relevant scale. The Lyapunov exponents are found to obey the relationship of  $\lambda_L \sim \kappa T$ . The unitary Fermi gas is another example with scaling invariance. With the properties of highly controllable and hyper clean it can be a perfect playground to investigate the information scrambling[25, 26] and thermalization in closed quantum systems. At the unitary point, the non-relativistic conformal symmetry emerges and investigations have been taken to discuss its duality to a gravity theory[27, 28]. The behaviors of the Lyapunov exponent have been studied at both high tem-

\* boyangleo@gmail.com

perature and low temperature limits [29]. However, it is more interesting to investigate the behavior around the critical temperature, where it has been shown more close to a non-Fermi liquid behavior[30–33].

In this work, we calculate the Lyapunov exponent of a  $N$ -flavor Fermi gas with tunable interaction. The OTOC is evaluated by a series of ladder diagrams and the Lyapunov exponent is calculated to the order of  $1/N$ . As the interaction strength increases from the BCS limit to the unitary regime we find that the Lyapunov exponent monotonically increases while the temperature is fixed. We also investigate the temperature dependence of the Lyapunov exponent at the unitarity.  $\lambda_L$  can increase to  $\lambda_L \sim T$  for  $N = 1$  case when the temperature is close to the critical temperature. Furthermore, we also find that the Lyapunov exponent behaves as  $\lambda_L \propto za_s^2 T^2/N$  for high temperature at the BSC limit, where  $a_s \rightarrow 0^-$ .

## II. MODEL

We will start from a system with  $N$  fermion flavors. The Hamiltonian can be cast as

$$\hat{H} = \int d^3\mathbf{r} \left\{ \sum_{i\sigma} \hat{\psi}_{i\sigma}^\dagger(\mathbf{r}) \left( -\frac{\nabla^2}{2m} - \mu \right) \hat{\psi}_{i\sigma}(\mathbf{r}) - \frac{g}{N} \sum_{ij} \hat{\psi}_{i\uparrow}^\dagger(\mathbf{r}) \hat{\psi}_{i\downarrow}^\dagger(\mathbf{r}) \hat{\psi}_{j\downarrow}(\mathbf{r}) \hat{\psi}_{j\uparrow}(\mathbf{r}) \right\}, \quad (1)$$

where  $\psi_{i\sigma}(\psi_{i\sigma}^\dagger)$  is the annihilation(creation) operator of the fermion field with flavor  $i$  and spin  $\sigma$ . Parameter  $g$  is the bare interaction strength between the fermions. Here we assume the interaction strengths between different flavors are the same, and it can be related to a s-wave scattering length  $a_s$  by the following renormalization relation

$$\frac{1}{g} = -\frac{m}{4\pi a_s} + \int \frac{d^3\mathbf{k}}{(2\pi)^3} \frac{1}{2\epsilon_{\mathbf{k}}}, \quad (2)$$

where  $\epsilon_{\mathbf{k}} = k^2/2m$ , and  $m$  is the mass of the fermions. By introducing an auxiliary bosonic field  $\varphi$  the four-fermion interaction term can be decoupled through the Hubbard-stratonovich transformation. Then in the imaginary time path integral formulism the partition function can be written as  $\mathcal{Z} = \int \mathcal{D}[\psi_{i\sigma}, \psi_{i\sigma}^\dagger, \varphi, \bar{\varphi}] e^{-S[\psi_{i\sigma}, \psi_{i\sigma}^\dagger, \varphi, \bar{\varphi}]}$ , where the action  $S$  is

$$S[\psi_{i\sigma}, \psi_{i\sigma}^\dagger, \varphi, \bar{\varphi}] = \int d\tau d^3\mathbf{r} \left( \sum_{i\sigma} \psi_{i\sigma}^\dagger(\tau, \mathbf{r}) \left( \partial_\tau - \frac{\nabla^2}{2m} - \mu \right) \psi_{i\sigma}(\tau, \mathbf{r}) - \sum_i \varphi \psi_{i\uparrow}^\dagger \psi_{i\downarrow}^\dagger - \sum_i \bar{\varphi} \psi_{i\downarrow} \psi_{i\uparrow} + \frac{N\bar{\varphi}\varphi}{g} \right). \quad (3)$$

In this work we set  $\hbar = 1$ .

The imaginary time Greens' functions of fermion and boson are defined as  $\delta_{ij}\delta_{\sigma\sigma'} G(\tau, \mathbf{r}) = \langle \psi_{i\sigma}^\dagger(\tau, \mathbf{r}) \psi_{j\sigma'}(0, 0) \rangle$

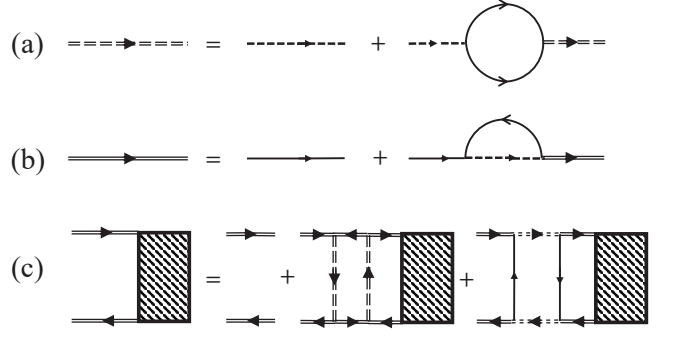


FIG. 2. (a) The Feynman diagram of the Dyson-Schwinger equation for field  $\varphi$ . (b) The Feynman diagram of the Dyson-Schwinger equation for field  $\psi_{i\sigma}$ . The double solid (dashed) line and the solid (dashed) line represent the dressed and free propagators of  $\psi_{i\sigma}(\varphi)$ , respectively. (c) The Feynman diagram of the Bethe-Salpeter equation of the out-of-time-ordered correlator.

and  $\mathcal{G}(\tau, \mathbf{r}) = \langle \bar{\varphi}(\tau, \mathbf{r}) \varphi(0, 0) \rangle$ , respectively. In the momentum space the free propagators can be simply expressed as

$$G^{(0)}(i\omega_n^f, \mathbf{k}) = \frac{1}{i\omega_n - \epsilon_{\mathbf{k}} + \mu}, \quad G^{(0)}(i\omega_n^b, \mathbf{k}) = g/N, \quad (4)$$

where  $\omega_n^f = (2n+1)\pi/\beta$  and  $\omega_n^b = 2n\pi/\beta$  are the Matsubara frequencies for fermions and bosons, respectively, and  $\beta = 1/k_B T$ . In order to calculate the Lyapunov exponent up to the order of  $1/N$  we will involve the dressed propagators of fields  $\psi$  and  $\varphi$  as shown in Fig. 2. The dressed propagator of  $\varphi$  is a resummation of bubble diagram. Then, it's written as

$$\mathcal{G}(i\omega_n^b, \mathbf{k}) = \frac{g/N}{1 - g\Pi(i\omega_n^b, \mathbf{k})}, \quad (5)$$

where  $\Pi(i\omega_n^b, \mathbf{k})$  is the one-loop bubble

$$\Pi(i\omega_n^b, \mathbf{q}) = \int \frac{d^3\mathbf{k}}{(2\pi)^3} \frac{1 - n_F(\epsilon_{\mathbf{k}} - \mu) - n_F(\epsilon_{\mathbf{q}-\mathbf{k}} - \mu)}{-i\omega_n^b + \epsilon_{\mathbf{k}} + \epsilon_{\mathbf{q}-\mathbf{k}} - 2\mu}. \quad (6)$$

$n_F(\epsilon_{\mathbf{k}} - \mu) = 1/\exp(\beta(\epsilon_{\mathbf{k}} - \mu) + 1)$  is the Fermi-Dirac distribution function. The dressed propagator of field  $\psi_i$  is

$$G(i\omega_n^f, \mathbf{k}) = \frac{1}{-i\omega_n^f + \epsilon_{\mathbf{k}} - \mu - \Sigma(i\omega_n^f, \mathbf{k})}, \quad (7)$$

where the self-energy of fermions  $\Sigma(i\omega_n^f, \vec{k})$  is expressed as

$$\Sigma(i\omega_n^f, \mathbf{k}) = \frac{1}{\beta} \sum_{\omega_m^b} \int \frac{d^3\mathbf{q}}{(2\pi)^3} \frac{\mathcal{G}(i\omega_m^b, \mathbf{q})}{-i\omega_m^b + i\omega_n^f + \epsilon_{\mathbf{q}-\mathbf{k}} - \mu}. \quad (8)$$

The corresponding retarded Green's functions are defined as usual as  $\delta_{ij}\delta_{\sigma\sigma'} G_R(t, \mathbf{r}) =$

$-i\theta(t)\langle\{\psi_{i\sigma}(t, \mathbf{r}), \psi_{j\sigma'}^\dagger(0, 0)\}\rangle$  and  $\mathcal{G}_R(t, \vec{r}) = -i\theta(t)\langle[\varphi(t, \vec{r}), \bar{\varphi}(0, 0)]\rangle$ , where  $\theta(t)$  is the heaviside step function. In momentum space the forms of the retarded Green's functions can be obtained by the analytic continuation of the Eq.(5) and (7) as  $\mathcal{G}_R(\omega, \mathbf{k}) = \mathcal{G}(i\omega_n^b \rightarrow \omega + i0^+, \mathbf{k})$  and  $G_R(\omega, \mathbf{k}) = G(i\omega_n^f \rightarrow \omega + i0^+, \mathbf{k})$ . Then  $G_R(\omega, \mathbf{k})$  is written as

$$G_R(\omega, \mathbf{k}) = \frac{1}{-\omega - i0^+ + \epsilon_{\mathbf{k}} - \mu - \Sigma(\omega + i0^+, \mathbf{k})}. \quad (9)$$

Hence, in the dressed retarded Green's function the pole is modified by the self-energy. Working to the first order in  $\Sigma$  the pole can be approximately calculated as  $\omega^* = \epsilon_{\mathbf{k}} - \mu - \text{Re}\Sigma(\epsilon_{\mathbf{k}} - \mu + i0^+, \mathbf{k}) + i\Gamma(k)$ , and the quantum scattering rate  $\Gamma(k)$  is defined as  $\Gamma(k) \equiv -\text{Im}\Sigma(\epsilon_{\mathbf{k}} - \mu + i0^+, \mathbf{k})$ .

In order to evaluate the OTOC we need to define the symmetrized Wightman function as

$$\begin{aligned} \delta_{ij}\delta_{\sigma\sigma'}G_W(t, \mathbf{r}) &= \text{Tr}\{\sqrt{\rho}\psi_{i\sigma}(t, \mathbf{r})\sqrt{\rho}\psi_{i\sigma'}^\dagger(0, 0)\}, \\ G_W(t, \mathbf{r}) &= \text{Tr}\{\sqrt{\rho}\varphi(t, \mathbf{r})\sqrt{\rho}\bar{\varphi}(0, 0)\}. \end{aligned} \quad (10)$$

In the momentum space they can be written in terms of the spectral functions of fields  $\psi_{i\sigma}$  and  $\varphi$  as

$$\begin{aligned} G_W(\omega, \mathbf{k}) &= \frac{A_F(\omega, \mathbf{k})}{2\cosh(\omega\beta/2)}, \\ \mathcal{G}_W(\omega, \mathbf{k}) &= \frac{A_B(\omega, \mathbf{k})}{2\sinh(\omega\beta/2)}, \end{aligned} \quad (11)$$

The spectral functions can be calculated as the imaginary parts of the retarded Green's functions,  $A_F(\omega, \mathbf{k}) = -2\text{Im}G_R(\omega, \mathbf{k})$  and  $A_B(\omega, \mathbf{k}) = -2\text{Im}\mathcal{G}_R(\omega, \mathbf{k})$ .

### III. THE LYAPUNOV EXPONENT

In order to calculate the Lyapunov exponent it's convenient to evaluate the "regulated" squared anti-commutator defined as [19, 24]

$$\begin{aligned} \mathcal{C}(t) &= \frac{\theta(t)}{2N^2} \sum_{i,j,\sigma} \int d^3\mathbf{r} \text{Tr} \left[ \sqrt{\rho}\{\psi_{i\sigma}(t, \mathbf{r}), \psi_{j\sigma}^\dagger(0, 0)\} \right. \\ &\quad \left. \times \sqrt{\rho}\{\psi_{i\sigma}(t, \mathbf{r}), \psi_{j\sigma}^\dagger(0, 0)\}^\dagger \right]. \end{aligned}$$

The factor  $1/2N^2$  is to normalized the summation of indices  $i, j$  and  $\sigma$ . At the moment of  $t = 0$  the anti-commutator vanishes because of  $\mathbf{r} \neq 0$ . However, in chaotic system the time evolution of the operators may involve increasing degree of freedoms. As a result the fields become nonlocal at later time. It is conjectured that the squared anti-commutator will have an exponential growth  $\mathcal{C}(t) \sim e^{\lambda_L t}$  at short time. Analogously to the approach in ref. [18], in order to compute the  $\lambda_L$  to the leading order in  $1/N$  we only keep the fastest-growing diagrams, which is a set of ladder diagrams as shown in Fig.2 (c). The "rails" of the ladder correspond to the retarded Green's functions. They are defined on

the two real time folds. The two rails are separated by an imaginary time difference  $i\beta/2$  and they are connected by "rungs". The "rungs" correspond to the Wightman Green's functions. The ladder diagrams can be summarized as two types of two-rung diagrams as in Fig.2 (c). In type I the two rungs are the Wightman Green's functions of field  $\varphi$ , while in type II the two rungs are the Wightman Green's functions of field  $\psi$ .

The Fourier transformation of  $\mathcal{C}(t)$  is denoted as  $\mathcal{C}(\omega)$  with  $\mathcal{C}(t) = \int d\omega e^{-i\omega t} \mathcal{C}(\omega)$ . To sum up all the ladder series it's convenient to define a function  $f(\nu; \omega, \mathbf{k})$  as

$$\mathcal{C}(\nu) = \frac{1}{N} \int \frac{d\omega d^3\mathbf{k}}{(2\pi)^4} f(\nu; \omega, \mathbf{k}). \quad (12)$$

The lowest order of  $f(\nu; \omega, \mathbf{k})$  is simply expressed as  $G_R(\omega, \mathbf{k})G_R^*(\omega - \nu, \mathbf{k})$ . Summation of all the ladder diagrams yields the Bethe-Salpeter equation

$$\begin{aligned} f(\nu; \omega, \mathbf{k}) &= \\ G_R(\omega, \mathbf{k})G_R^*(\omega - \nu, \mathbf{k}) &\left(1 + \int \frac{d\omega' d^3\mathbf{k}'}{(2\pi)^4} \right. \\ &\left. (\mathcal{K}_1(\nu; \omega, \mathbf{k}; \omega', \mathbf{k}') + \mathcal{K}_2(\nu; \omega, \mathbf{k}; \omega', \mathbf{k}')) f(\nu; \omega', \mathbf{k}')\right), \end{aligned} \quad (13)$$

where  $\mathcal{K}_1$  and  $\mathcal{K}_2$  are the integral kernels corresponding to the type I and type II two-rung diagrams in Fig.2 (c), respectively. They can be written as

$$\begin{aligned} \mathcal{K}_1(\nu; \omega, \mathbf{k}; \omega', \mathbf{k}') &= \\ &\int \frac{d\omega'' d^3\mathbf{k}''}{(2\pi)^4} G_R(\omega'', \mathbf{k}'')G_R^*(\omega'' + \nu, \mathbf{k}'') \\ &\times \mathcal{G}_W(\omega + \omega'', \mathbf{k} + \mathbf{k}'')\mathcal{G}_W(\omega' + \omega'', \mathbf{k}' + \mathbf{k}''), \\ \mathcal{K}_2(\nu; \omega, \mathbf{k}; \omega', \mathbf{k}') &= \\ &N \int \frac{d\omega'' d^3\mathbf{k}''}{(2\pi)^4} \mathcal{G}_R(\omega'', \mathbf{k}'')\mathcal{G}_R^*(\omega'' - \nu, \mathbf{k}'') \\ &\times G_W(\omega + \omega'', \mathbf{k} + \mathbf{k}'')G_W(\omega' + \omega'', \mathbf{k}' + \mathbf{k}''). \end{aligned} \quad (14)$$

For the following calculation we will take several approximations. Firstly, one expects that the  $f(\nu; \omega, \mathbf{k})$  to be exponentially growing, while inhomogeneous term in Eq. (13) will be decaying. Hence, the inhomogeneous term can be safely dropped here without affecting the evaluation of the growth rate. Secondly, the pair of fermionic Green's functions  $G_R(\omega, \mathbf{k})G_R^*(\omega - \nu, \mathbf{k})$  in Eq. (13) can be approximated as  $\frac{2\pi i \delta(\omega - \epsilon_{\mathbf{k}} + \mu)}{\nu + 2i\Gamma(k)}$ . Thirdly, because in the above approximation all pairs of the retarded Green's functions include a on-shell delta function, it's natural to postulate the on-shell form of  $f(\nu; \omega, \mathbf{k})$  as  $f(\nu; \omega, \mathbf{k}) \approx f(\nu; \mathbf{k})\delta(\omega - \epsilon_{\mathbf{k}} + \mu)$ [18, 19]. Please refer to the appendix A for the details of the approximation. With all above approximations the Bethe-Salpeter equation of Eq.(13) can be reduced to

$$\begin{aligned} (-i\omega + 2T\tilde{\Gamma}(\tilde{k}))f(\omega; \tilde{k}) &= \\ \frac{T}{N} \int \frac{d\tilde{k}' \tilde{k}'}{\tilde{k}} &\left(\tilde{\mathcal{K}}_1(\tilde{k}, \tilde{k}') + \tilde{\mathcal{K}}_2(\tilde{k}, \tilde{k}')\right)f(\omega; \tilde{k}'), \end{aligned} \quad (15)$$

where the momenta have been rescaled to be dimensionless as  $\tilde{k} = k/\sqrt{T}$  and  $\tilde{k}' = k'/\sqrt{T}$ . Correspondingly we

define a dimensionless quantum scattering rate  $\tilde{\Gamma} = \Gamma/T$ . Here we have assumed the function  $f(\omega, \mathbf{k})$  is rotationally invariant and integrated over the angles. Then the function  $f(\omega, \mathbf{k})$  is reduced to  $f(\omega, k)$  in Eq. (15). The dimensionless functions  $\tilde{\mathcal{K}}_1$  and  $\tilde{\mathcal{K}}_2$  are written as

$$\begin{aligned}\tilde{\mathcal{K}}_1(\tilde{k}, \tilde{k}') &= N \int \frac{d\tilde{k}''}{64\pi^5} \frac{1}{\tilde{\Gamma}(\tilde{k}'')} I(\tilde{k}, \tilde{k}'') I(\tilde{k}', \tilde{k}''), \\ \tilde{\mathcal{K}}_2(\tilde{k}, \tilde{k}') &= N^2 \int \frac{d\tilde{k}'' d\tilde{\omega}''}{128\pi^5} \frac{|\tilde{\mathcal{G}}_R(\tilde{\omega}'', \tilde{k}'')|^2 \Theta(\tilde{k}, \tilde{k}', \tilde{k}'')}{\cosh(\frac{\tilde{\epsilon}_k - \tilde{\mu} - \tilde{\omega}''}{2}) \cosh(\frac{\tilde{\epsilon}_{k'} - \tilde{\mu} - \tilde{\omega}''}{2})},\end{aligned}\quad (16)$$

where  $\tilde{k}'' = k''/\sqrt{T}$ ,  $\tilde{\omega}'' = \omega''/T$ ,  $\tilde{\epsilon}_k = \epsilon_k/T$  and  $\tilde{\mu} = \mu/T$  and the bosonic retarded Green's functions are also rescaled to be dimensionless by  $\tilde{\mathcal{G}}_R = \sqrt{T}\mathcal{G}_R$ . The  $\Theta$  function is defined as  $\Theta(k, k', k'') = \theta(2k'k'' + \epsilon_{\mathbf{k}''} - \mu + k''^2)\theta(2k'k'' - \epsilon_{\mathbf{k}''} + \mu - k''^2)\theta(2kk'' + \epsilon_{\mathbf{k}''} - \mu + k''^2)\theta(2kk'' - \epsilon_{\mathbf{k}''} + \mu - k''^2)$ . The dimensionless function  $I(\tilde{k}', \tilde{k}'')$  is defined as

$$I(\tilde{k}', \tilde{k}'') = \int_{|\tilde{k}' - \tilde{k}''|}^{\tilde{k}' + \tilde{k}''} \tilde{p} d\tilde{p} \tilde{\mathcal{G}}_W(\tilde{\epsilon}_{k'} + \tilde{\epsilon}_{k''} - 2\tilde{\mu}, \tilde{p}). \quad (17)$$

To more easily solve for the Lyapunov exponent the Bethe-Salpeter equation of Eq. (15) can be written in a simply form

$$-i\omega\mathcal{F}(\omega; \tilde{k}) = \frac{T}{N} \int d\tilde{k}' \mathcal{S}(\tilde{k}, \tilde{k}') \mathcal{F}(\omega; \tilde{k}'). \quad (18)$$

where  $\mathcal{F}(\omega; \tilde{k}) = \tilde{k}f(\omega; \tilde{k})$  and the dimensionless integral kernel  $\mathcal{S}(\tilde{k}, \tilde{k}')$  is defined as following

$$\mathcal{S}(\tilde{k}, \tilde{k}') = \tilde{\mathcal{K}}_1(\tilde{k}, \tilde{k}') + \tilde{\mathcal{K}}_2(\tilde{k}, \tilde{k}') - N\tilde{\Gamma}(\tilde{k}')\delta(\tilde{k} - \tilde{k}'). \quad (19)$$

We do not know how to solve Eq. (18) analytically. However, it can be solved numerically by discretizing the momenta  $\tilde{k}$  and  $\tilde{k}'$  in the integral kernel  $\mathcal{S}(\tilde{k}, \tilde{k}')$ . Then, the integral becomes the summation over the discrete momentum and Eq. (18) can be written as

$$-i\omega\mathcal{F}(\omega; \tilde{k}_i) = \frac{T}{N} \sum_{\tilde{k}_j} \mathcal{S}(\tilde{k}_i, \tilde{k}_j) \mathcal{F}(\omega; \tilde{k}_j), \quad (20)$$

where  $\tilde{k}_i$  is the discrete momentum with a small intervals. Obviously  $-i\omega$  is given by the eigenvalues of the kernel  $\mathcal{S}(\tilde{k}_i, \tilde{k}_j)$  multiplied by a factor  $T/N$ . The Lyapunov exponent corresponds to the largest eigenvalue. Please refer to the appendix B for the details of the numerical calculation of the Lyapunov exponent.

#### IV. QUANTUM CHAOS AT THE UNITARY POINT

In this section we study the case of unitary Fermi gases by setting  $N = 1$ . This is not a fully controllable choice.

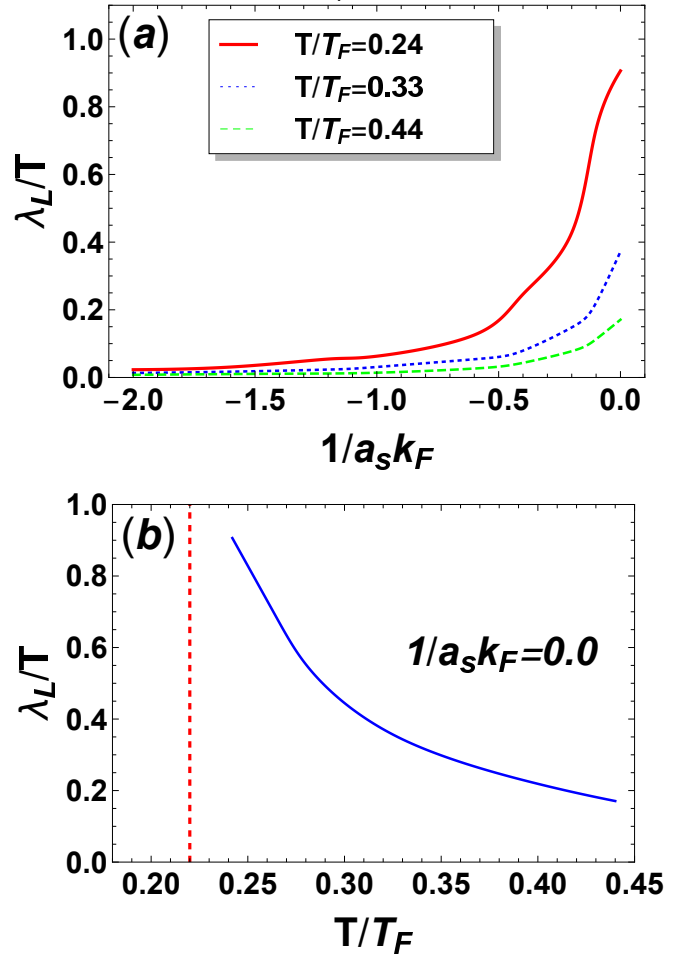


FIG. 3. (Color online) (a)  $\lambda_L/T$  as a function of  $1/a_s k_F$ . The red solid, the blue dotted and the green dashed curves correspond to different temperatures  $T/T_F = 0.24, 0.33$  and  $0.44$ , respectively. (b)  $\lambda_L/T$  as a function of temperature  $T/T_F$  for case of  $1/a_s k_F = 0$ .

However, since we only focus on the variations of the Lyapunov exponent with respect to the scattering length  $a_s$  and the temperature, it may generate qualitative correct interpretation as the large  $N$  cases and inspire useful insight. In Fig. 3 (a) we plot  $\lambda_L/T$  as a function of  $1/a_s k_F$  for fixed temperature  $T/T_F = 0.24, 0.33$  and  $0.44$ . If we compare these temperatures with the critical temperature calculated in the Nozières and Schmitt-Rink (NSR) scheme [34, 35], which is  $T_c = 0.22T_F$  at  $1/a_s k_F = 0$ , they can be written as  $T/T_c = 1.1, 1.5$ , and  $2.0$ . One observes that the Lyapunov exponent monotonically increases as  $1/a_s k_F$  goes from the BCS limit to the unitary regime. For lower temperature the  $\lambda_L$  increases much faster than the higher temperature cases. At the unitary point  $1/a_s k_F = 0$  we plot  $\lambda_L/T$  as a function of temperature  $T/T_F$  in Fig. 3 (b). As the temperature drops the Lyapunov exponent monotonically increases and approaches the upper bound  $2\pi T$ . At the temperature of  $T/T_F = 0.24$ , which corresponds to  $T/T_c = 1.1$  the Lyapunov exponent is approximately  $0.9 \times 2\pi T$ .

punov exponent can reach a value of  $\lambda_L \approx 0.9T$ .

At the unitary point and temperature close to the critical point the system possesses two features. First, the system is scaling invariant. It obeys the non-relativistic conformal symmetry (the Schrödinger group). Investigations have been taken for the possible non-relativistic version of ADS/CFT duality [27, 28]. Second, it has been shown that around the critical temperature the system demonstrate a behavior of non-Fermi liquid due to the strong pairing fluctuations [30–33]. Several researches has shown that certain systems lacking of quasi-particle excitations demonstrate strong chaos [19, 23, 24, 36, 37]. Hence, it's not surprising that our system scrambles the fastest at the unitarity and the temperature close to  $T_c$ .

## V. THE BEHAVIORS IN THE BCS LIMIT

At the BCS limit the scattering length  $a_s \rightarrow 0^-$ . The retarded Green's function  $\mathcal{G}_R$  of the field  $\varphi$  can be expanded in terms of small  $a_s$  as the following

$$\begin{aligned} \mathcal{G}_R(\omega, \mathbf{k}) &= \frac{1/N}{-\frac{m}{4\pi a_s} + \int \frac{d^3\mathbf{k}}{(2\pi)^3} \frac{1}{2\epsilon_{\mathbf{k}}} - \int \frac{d^3\mathbf{k}}{(2\pi)^3} \frac{1-n_F(\epsilon_{\mathbf{k}}-\mu)-n_F(\epsilon_{\mathbf{q}-\mathbf{k}}-\mu)}{-\omega-i0^++\epsilon_{\mathbf{k}}+\epsilon_{\mathbf{q}-\mathbf{k}}-2\mu}} \\ &\propto a_s/N. \end{aligned} \quad (21)$$

Notice that the temperature must be far from the critical temperature. Otherwise, according to the Thouless criterion one has  $-\frac{m}{4\pi a_s} + \int \frac{d^3\mathbf{k}}{(2\pi)^3} \frac{1}{2\epsilon_{\mathbf{k}}} - \int \frac{d^3\mathbf{k}}{(2\pi)^3} \frac{1-n_F(\epsilon_{\mathbf{k}}-\mu)-n_F(\epsilon_{\mathbf{q}-\mathbf{k}}-\mu)}{-\omega+\epsilon_{\mathbf{k}}+\epsilon_{\mathbf{q}-\mathbf{k}}-2\mu} \rightarrow 0$  when  $T$  approaches  $T_c$  and  $\mathcal{G}_R$  can not be expanded for small  $a_s$ . Furthermore, since the Wightman function  $\mathcal{G}_W$  the quantum scattering rate  $\Gamma(k)$  can be calculated by  $\mathcal{G}_W(\omega, \mathbf{k}) = \frac{-\text{Im} \mathcal{G}_R(\omega, \mathbf{k})}{\sinh(\omega\beta/2)}$  and  $\Gamma(k) = \int \frac{d^3\mathbf{q}}{2(2\pi)^3} \mathcal{G}_W(\epsilon_{\mathbf{k}} + \epsilon_{\mathbf{q}-\mathbf{k}} - 2\mu, \mathbf{q}) \frac{\cosh((\epsilon_{\mathbf{k}}-\mu)/2T)}{\cosh((\epsilon_{\mathbf{q}-\mathbf{k}}-\mu)/2T)}$ , their behaviors for small  $a_s$  can be easily derived as  $\mathcal{G}_R \propto za_s^2\sqrt{T}/N$  and  $\Gamma(k) \propto za_s^2T^2/N$ , where  $z \equiv \exp(\mu/T)$  is the fugacity. Please refer to Appendix C for the details.  $\tilde{\mathcal{K}}_1(\tilde{k}, \tilde{k}')$  and  $\tilde{\mathcal{K}}_2(\tilde{k}, \tilde{k}')$  in the integral kernel of Eq. (19) are functions of  $\mathcal{G}_R$  and  $\mathcal{G}_W$  as shown in Eq. (16). Then it's straight forward to obtain the behaviors as  $\tilde{\mathcal{K}}_1(\tilde{k}, \tilde{k}') \propto za_s^2T$  and  $\tilde{\mathcal{K}}_2(\tilde{k}, \tilde{k}') \propto za_s^2T$ . The three terms in Eq. (19) are all have the same asymptotic form of  $za_s^2T$ . Hence, as  $a_s \rightarrow 0^-$  the Lyapunov exponent behaves as  $\lambda_L \propto za_s^2T^2/N$ , which is consistent with the investigations on the Fermi liquid theory with well defined quasi-particles [29, 38, 39].

## VI. CONCLUSIONS

We have computed the Lyapunov exponent for a N-flavor Fermion system using  $1/N$  expansion. The variation of the Lyapunov exponent with respect to the scattering length  $a_s$  and the temperature  $T$  has been investigated. When  $T$  is fixed the Lyapunov exponent monotonically increases as the  $1/a_s k_F$  increases from the BCS

limit to the unitary regime. When the scattering length is fixed to  $1/a_s k_F = 0$  the Lyapunov exponent increases while the temperature drops. Around the critical temperature it can reach to the order of  $\lambda_L \sim T$  for  $N = 1$  case. Basically, our results indicate that with strong pairing fluctuations the system exhibits strong chaos. Furthermore, the behavior of  $\lambda_L$  at the BCS limit was calculated as  $\lambda_L \propto za_s^2T^2/N$ , which is consistent with the Fermi liquid theory.

## VII. ACKNOWLEDGEMENTS

We thank Shizhong Zhang and Yu Chen for very helpful discussions. The work is supported by the National Science Foundation of China (Grant No. NSFC-11874002), Beijing Natural Science Foundation (Grand No. Z180007) and Hong Kong Research Grants Council, GRF 17304719, CRF C6026-16W and C6005-17G.

### Appendix A: Approximations for the reduction of Eq. (15)

With the first approximation the inhomogeneous term is dropped. Then the Eq. (13) is reduced to

$$\begin{aligned} f(\nu; \omega, \mathbf{k}) &\approx G_R(\omega, \mathbf{k}) G_R^*(\omega - \nu, \mathbf{k}) \int \frac{d\omega' d^3\mathbf{k}'}{(2\pi)^4} \\ &(\mathcal{K}_1(\nu; \omega, \mathbf{k}; \omega', \mathbf{k}') + \mathcal{K}_2(\nu; \omega, \mathbf{k}; \omega', \mathbf{k}')) f(\nu; \omega', \mathbf{k}'). \end{aligned} \quad (A1)$$

The second approximation is performed on the pair propagators  $G_R(\omega, \mathbf{k}) G_R^*(\omega - \nu, \mathbf{k})$ . In the free fermion case it's expressed as

$$G_R(\omega, \mathbf{k}) G_R^*(\omega - \nu, \mathbf{k}) = \frac{1}{\omega - \epsilon_{\mathbf{k}} + \mu + i0^+} \frac{1}{\omega - \nu - \epsilon_{\mathbf{k}} + \mu - i0^+}. \quad (A2)$$

The integration over  $\omega$  can be evaluated by the method of residue. Then it's straight forward to yield

$$G_R(\omega, \mathbf{k}) G_R^*(\omega - \nu, \mathbf{k}) = \frac{2\pi i \delta(\omega - \epsilon_{\mathbf{k}} + \mu)}{\nu + 2i0^+}. \quad (A3)$$

The approximation is taken by replacing the  $0^+$  by the scattering rate  $\Gamma(k)$  for the interacting case. Then,

$$G_R(\omega, \mathbf{k}) G_R^*(\omega - \nu, \mathbf{k}) = \frac{2\pi i \delta(\omega - \epsilon_{\mathbf{k}} + \mu)}{\nu + 2i\Gamma(k)}. \quad (A4)$$

As discussed in the maintext the third approximation is to postulate the on-shell form  $f(\nu; \omega, \mathbf{k}) \approx f(\nu; \mathbf{k}) \delta(\omega - \epsilon_{\mathbf{k}} + \mu)$ . Then the Eq. (A1) can be written as

$$\begin{aligned} (-i\nu + 2\Gamma(k)) f(\nu; \mathbf{k}) &= \int \frac{d\omega' d^3\mathbf{k}'}{(2\pi)^4} (\mathcal{K}_1(\nu; \omega, \mathbf{k}; \omega', \mathbf{k}') \\ &+ \mathcal{K}_2(\nu; \omega, \mathbf{k}; \omega', \mathbf{k}')) 2\pi \delta(\omega - \epsilon_{\mathbf{k}} + \mu) f(\nu; \mathbf{k}'), \end{aligned} \quad (A5)$$

Assuming  $f(\nu; \mathbf{k}')$  is rotationally invariant and performing the integration by implementing the delta function  $\delta(\omega - \epsilon_{\mathbf{k}} + \mu)$  one obtains the Eq. (15).

## Appendix B: Remarks on Numerical technique

To numerically solve for the Lyapunov exponent we first discretize the momenta  $k$  and  $k'$  of the integral kernel  $\mathcal{S}(k, k')$  in Eq. (19) into  $N_{size}$  pieces. The cutoffs of momenta  $k$  and  $k'$  are set to  $\Lambda = 15$ . We have also checked the convergence of the results by performing the calculation for larger cutoffs. The kernel  $\mathcal{S}(k, k')$  is symmetric for exchanging  $k$  and  $k'$ . Then it can be easily diagonalized to obtain the eigenvalues, which are denoted as  $\lambda_i$  here. The Lyapunov exponent is related to the largest eigenvalue as  $\lambda_L N/T = \max(\lambda_i)$ . Then the same calculation is performed for different  $N_{size}$  and the corresponding value of  $\lambda_L N/T$  is obtained. As an example we illustrate the case of  $1/a_s k_F = 0$  and  $T/T_F = 0.24$  in Fig. 4. The final value of  $\lambda_L N/T$  is read by the extrapolation to  $1/N_{size} = 0$ .

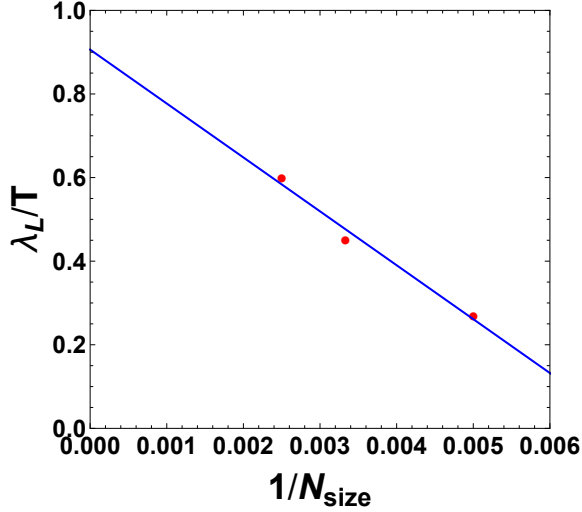


FIG. 4. (Color online) The extrapolation of  $\lambda_L/T$  as a function of the discretized interval  $1/N_{size}$ . This plot is for the case of  $1/a_s k_F = 0$  and  $T/T_F = 0.24$ .

## Appendix C: Behaviors at BCS limit

At the BCS limit one has  $a_s^{-1} \rightarrow -\infty$ . Then the asymptotic behaviors of various propagators and the scattering rate  $\Gamma(k)$  are demonstrated as the following. The full propagator of field  $\varphi$  is

$$\mathcal{G}_R(\omega, \mathbf{k}) = \frac{1/N}{1/g - \Pi(\omega, \mathbf{k})} \equiv \frac{1/N}{Re + iIm}, \quad (C1)$$

where

$$\begin{aligned} Re &= -\frac{m}{4\pi a_s} + \int \frac{d^3\mathbf{k}}{(2\pi)^3} \frac{1}{2\epsilon_{\mathbf{k}}} \\ &\quad - \int \frac{d^3\mathbf{k}}{(2\pi)^3} \frac{1 - n_F(\epsilon_{\mathbf{k}} - \mu) - n_F(\epsilon_{\mathbf{q}-\mathbf{k}} - \mu)}{-\omega + \epsilon_{\mathbf{k}} + \epsilon_{\mathbf{q}-\mathbf{k}} - 2\mu} \\ Im &= -\pi \int \frac{d^3\mathbf{k}}{(2\pi)^3} (1 - n_F(\epsilon_{\mathbf{k}} - \mu) - n_F(\epsilon_{\mathbf{q}-\mathbf{k}} - \mu)) \end{aligned}$$

$$\delta(-\omega + \epsilon_{\mathbf{k}} + \epsilon_{\mathbf{q}-\mathbf{k}} - 2\mu). \quad (C2)$$

After we rescale all the momenta and frequency by  $\mathbf{k} \rightarrow \mathbf{k}/\sqrt{T}$ ,  $\mathbf{q} \rightarrow \mathbf{q}/\sqrt{T}$  and  $\omega \rightarrow \omega/T$  it's straight forward to get the following asymptotic behaviors for large  $a_s^{-1}$

$$\begin{aligned} Re &\propto a_s^{-1}, \\ Im &\propto \sqrt{T}. \end{aligned} \quad (C3)$$

Notice that the temperature here must be far from the superfluid critical temperature, otherwise  $Re \rightarrow 0$ . Then for large  $a_s^{-1}$  the propagator  $\mathcal{G}_R(\omega, \mathbf{k})$  behaves as

$$\mathcal{G}_R(\omega, \mathbf{k}) \propto a_s/N. \quad (C4)$$

The imaginary part of  $\mathcal{G}_R(\omega, \mathbf{k})$  is

$$Im \mathcal{G}_R(\omega, \mathbf{k}) = -\frac{1}{N} \frac{Im}{Re^2 + Im^2} \propto a_s^2 \sqrt{T}/N. \quad (C5)$$

The Wightman function of field  $\varphi$  behaves as

$$\begin{aligned} \mathcal{G}_W(\omega_k - 2\mu, \mathbf{k}) &\equiv \frac{A_B(\omega_k - 2\mu, \mathbf{k})}{2 \sinh((\omega_k - 2\mu)\beta/2)} \\ &= \frac{-Im \mathcal{G}_R(\omega_k - 2\mu, \mathbf{k})}{\sinh((\omega_k - 2\mu)\beta/2)} \\ &\propto z a_s^2 \sqrt{T}/N. \end{aligned} \quad (C6)$$

The self-energy of fermions is

$$\Sigma(i\omega_n^f, \mathbf{k}) = \frac{1}{\beta} \sum_{\omega_m^b} \int \frac{d^3\mathbf{q}}{(2\pi)^3} \frac{\mathcal{G}(i\omega_m^b, \mathbf{q})}{-i\omega_m^b + i\omega_n^f + \epsilon_{\mathbf{q}-\mathbf{k}} - \mu}, \quad (C7)$$

where the summation over  $\omega_m^b$  is equivalent to a contour integration as the following

$$\begin{aligned} \Sigma(i\omega_n^f, \mathbf{k}) &= \int \frac{d^3\mathbf{q}}{(2\pi)^3} \left( \int \frac{dz}{2\pi i} \frac{n_B(z)(\mathcal{G}_R(z, \mathbf{q}) - \mathcal{G}_A(z, \mathbf{q}))}{-z + i\omega_n^f + \epsilon_{\mathbf{q}-\mathbf{k}} - \mu} \right. \\ &\quad \left. - \mathcal{G}(i\omega_n^f + \epsilon_{\mathbf{q}-\mathbf{k}} - \mu, \mathbf{q}) n_F(\epsilon_{\mathbf{q}-\mathbf{k}} - \mu) \right), \end{aligned} \quad (C8)$$

where  $\mathcal{G}_A$  is the advanced Green's function for field  $\varphi$ . After we take a analytical continuation the imaginary part of the self-energy can be calculated as

$$\begin{aligned} Im \Sigma(\omega + i0^+, \mathbf{k}) &= - \int \frac{d^3\mathbf{q}}{2(2\pi)^3} \left( n_F(\epsilon_{\mathbf{q}-\mathbf{k}} - \mu) A_B(\omega + \epsilon_{\mathbf{q}-\mathbf{k}} - \mu) \right. \\ &\quad \left. + \int dz A_B(z) \delta(-z + \omega + \epsilon_{\mathbf{q}-\mathbf{k}} - \mu) n_B(z) \right) \\ &= - \int \frac{d^3\mathbf{q}}{2(2\pi)^3} \mathcal{G}_W(\omega + \epsilon_{\mathbf{q}-\mathbf{k}} - \mu, \mathbf{q}) \frac{\cosh(\frac{\omega}{2T})}{\cosh(\frac{\epsilon_{\mathbf{q}-\mathbf{k}} - \mu}{2T})}. \end{aligned} \quad (C9)$$

The quantum scattering rate is defined as  $\Gamma(k) = -Im \Sigma(\epsilon_{\mathbf{k}} - \mu + i0^+, \mathbf{k})$ . Then it can be written as

$$\Gamma(k) = \int \frac{d^3\mathbf{q}}{2(2\pi)^3} \mathcal{G}_W(\epsilon_{\mathbf{k}} + \epsilon_{\mathbf{q}-\mathbf{k}} - 2\mu, \mathbf{q}) \frac{\cosh(\frac{\epsilon_{\mathbf{k}} - \mu}{2T})}{\cosh(\frac{\epsilon_{\mathbf{q}-\mathbf{k}} - \mu}{2T})}. \quad (C10)$$

As we have derived in Eq. (C6) the asymptotic behavior of the Wightman function is  $\mathcal{G}_W(\epsilon_{\mathbf{k}} + \epsilon_{\mathbf{q}-\mathbf{k}} - 2\mu, \mathbf{q}) \propto za_s^2\sqrt{T}/N$ , then the asymptotic behavior of the quantum scattering rate for large  $a_s^{-1}$  is as the following

$$\Gamma(k) \propto za_s^2 T^2 / N. \quad (\text{C11})$$

With all above asymptotic forms of  $\mathcal{G}_R(\omega, \mathbf{k})$ ,  $\mathcal{G}_W(\omega, \mathbf{k})$

and  $\Gamma(k)$  straight forward calculation yields

$$\begin{aligned} \tilde{\mathcal{K}}_1(\tilde{k}, \tilde{k}') &\propto za_s^2 T, \\ \tilde{\mathcal{K}}_2(\tilde{k}, \tilde{k}') &\propto za_s^2 T, \end{aligned} \quad (\text{C12})$$

and hence

$$\mathcal{S}(\tilde{k}, \tilde{k}') \propto za_s^2 T. \quad (\text{C13})$$

Then the asymptotic behavior of Laypunov exponent  $\lambda_L$  for large  $a_s^{-1}$  is

$$\lambda_L \propto T(za_s^2 T)/N = za_s^2 T^2 / N. \quad (\text{C14})$$

- 
- [1] Y. Sekino, L. Susskind, J. High Energy Phys. **2008**, 065 (2008).
  - [2] J. Maldacena, Advances in Theoretical and Mathematical Physics, vol. 2, no. 2, pp. 231, 1998, [International Journal of Theoretical Physics, vol. 38, article 1113, 1999].
  - [3] S. S. Gubser, I. R. Klebanov, and A. M. Polyakov, Physics Letters B, vol. 428, no. 1-2, pp. 105-114, 1998.
  - [4] E. Witten, Anti de Sitter space and holography, Advances in Theoretical and Mathematical Physics, vol. 2, no. 2, pp. 253-291, 1998.
  - [5] S.H. Shenker, D. Stanford, J. High Energy Phys. **2014**, 067 (2014).
  - [6] D. A. Roberts, D. Stanford, and L. Susskind, Localized shocks, Journal of High Energy Physics, vol. 1503, no. 51, 2015.
  - [7] S.H. Shenker, D. Stanford, J. High Energy Phys. **2015**, 132 (2015).
  - [8] A. Kitaev, Hidden correlations in the hawking radiation and thermal noise, talk given at Fundamental Physics Prize Symposium, in Proceedings of the Stanford SITP seminars, 2014.
  - [9] M. Rigol, V. Dunjko, and M. Olshanii, Thermalization and its mechanism for generic isolated quantum systems, Nature (London) 452, 854 (2008).
  - [10] T. Langen, R. Geiger, M. Kuhnert, B. Rauer, and J. Schmiedmayer, Local emergence of thermal correlations in an isolated quantum many-body system, Nat. Phys. 9, 640 (2013).
  - [11] A. M. Kaufman, M. E. Tai, A. Lukin, M. Rispoli, R. Schittko, P. M. Preiss, and M. Greiner, Quantum thermalization through entanglement in an isolated many-body system, Science 353, 794 (2016).
  - [12] A. I. Larkin, and Yu. N. Ovchinnikov, J. Exp. Theor. Phys. **28**, 1200 (1969).
  - [13] J. Maldacena, S. H. Shenker, and D. Stanford, J. High Energy Phys. **08** 106 (2016).
  - [14] G. Zhu, M. Hafezi, and T. Grover, Phys. Rev. A **94**, 062329 (2016).
  - [15] N. Y. Yao, F. Grusdt, B. Swingle, M. D. Lukin, D. M. Stamper-Kurn, J. E. Moore, E. Demler, arXiv:1607.01801(2016).
  - [16] M. Gättner, J. G. Bohnet, A. Safavi-Naini, M. L. Wall, J. J. Bollinger, and A. M. Rey, Nat. Phys. **13**, 781 (2017).
  - [17] J. Li, R. Fan, H. Wang, B. Ye, B. Zeng, H. Zhai, X. Peng, and J. Du, Phys. Rev. X. **7**, 031011 (2017).
  - [18] D. Stanford, J. High Energy Phys. **10**, 1007 (2016).
  - [19] D. Chowdhury, and B. Swingle, Phys. Rev. D. **96**, 065005 (2017).
  - [20] S. Sachdev, and J. Ye, Phys. Rev. Lett. **70**, 3339 (1993).
  - [21] A. Kitaev, A simple model of quantum holography. KITP <http://online.kitp.ucsb.edu/online/entangled15/kitaev/> (2015).
  - [22] J. Maldacena, D. Stanford, Phys. Rev. D. **94**, 106002 (2016).
  - [23] Aavishkar A. Patel and Subir Sachdev, Proc. Natl. Acad. Sci. **114**, 1844 (2017).
  - [24] S. Jian, and H. Yao, arXiv:1805.12299 (2018).
  - [25] G. Bentsen, T. Hashizume, A. S. Buyskikh, E. J. Davis, A. J. Daley, S. S. Gubser, and M. Schleier-Smith, Phys. Rev. Lett. **123**, 130601 (2019).
  - [26] C. B. Dağ, and L.-M. Duan, Phys. Rev. A **99**, 052322 (2019).
  - [27] K. Balasubramanian, and J. McGreevy, Phys. Rev. Lett. **101**, 061601 (2008).
  - [28] D. T. Son, Phys. Rev. D **78**, 046003 (2008).
  - [29] P. Zhang, Journal of Physics B: Atomic, Molecular and Optical Physics **52**, 13 (2019).
  - [30] S. Krinner, M. Lebrat, D. Husmann, C. Grenier, J.-P. Brantut, and T. Esslinger, Proc. Natl. Acad. Sci. USA **113**, 8144 (2016).
  - [31] B. Liu, H. Zhai, and S. Zhang, Phys. Rev. A **95**, 013623 (2017).
  - [32] D. Husmann, M. Lebrat, S. Häusler, J.-P. Brantut, L. Corman, and T. Esslinger, Proc. Natl. Acad. Sci. **115**, 8563 (2018).
  - [33] X. Han, B. Liu, and J. Hu, Phys. Rev. A **100**, 043604 (2019).
  - [34] P. Nozières and S. Schmitt-Rink, J. Low Temp. Phys. **59**, 195 (1985).
  - [35] Y. Ohashi, and A. Griffin, Phys. Rev. Lett. **89**, 130402 (2002).
  - [36] B. Swingle, and T. Senthil, Phys. Rev. B. **87**, 045123 (2013).
  - [37] S. A. Hartnoll, A. Lucas, and S. Sachdev, arXiv:1612.07324 (2018).
  - [38] Igor L. Aleiner, L. Faoro, and Lev B. Ioffe, Annals of Physics **375**, 378 (2016)
  - [39] S. Banerjee and E. Altman, Phys. Rev. B **95**, 134302 (2017).